

GRAPPA-accelerated high-resolution diffusion tensor imaging of infants without the need for general anesthesia

S. Skare¹, S. Holdsworth¹, K. Yeom¹, and R. Bammer¹

¹Radiology, Stanford University, Palo Alto, CA, United States

Introduction: At our institution, general anesthesia (GA) is used during MRI scans for children between 6 months and 5 years (in some cases even up to 15 y.o.), whereas for younger infants the "bundle-and-feed" technique is used. GA is associated with anesthesia-related health risks, increased cost and resource usage, and increased discomfort for the patient and parent. On the other hand, with the unsedated infant or child, excessive head motion is a significant problem, often leading to limited or non-diagnostic studies that need to be repeated. Over the past three years, over 1,200 adult stroke patients at our hospital have been acquired with our GRAPPA-accelerated diffusion-EPI sequence, along with tailored in-house made reconstruction software (1). This has led to substantial image quality improvements, including retrospective 3D motion correction, higher resolution, lowered Rician noise, and lower distortion and partial Fourier artifacts. While head motion in the adult population has appeared to be slow in nature and not too prevalent, the situation is the opposite for the unsedated infant. This has required further optimization of our diffusion method on unsedated infants and children to improve the diagnostic quality and potentially precluding the need for GA in selected patients.

Materials & Methods: Without sedation, two patients [A: 1-mo old male infant; B: 6-yr old male optical glioma patient] were imaged with our 3-shot DW-EPI sequence on a 1.5T GE Twin-speed system (Waukesha, WI) and an 8-channel head coil after informed parental consent was obtained. For both cases the scan parameters were as follows: 20 cm FOV, 192x192 acquisition matrix, 5 mm slice thickness, 0 mm gap, $b=1000$ s/mm². For patient A, a full DTI scan was acquired with 5 T_2w images followed by 35 isotropically distributed diffusion directions (1 NEX), whilst patient B was scanned with 1 $b=0$ (T_2w) and 3 x - y - z $b=1000$ s/mm² images (4 NEX). The total number of image volumes acquired (and to be realigned) for the two patients were (5+35)x3 = 120 (Pat. A) and (1+4)x4x3 = 60 (Pat. B). The scan time was minimized by avoiding peripheral gating as well as reference scans for Nyquist ghost correction and calibration scans for parallel imaging. As the child may move anytime, also during the acquisition of the T_2w data used for calibration, GRAPPA and ghost calibration information was calculated independently for all 4-5 T_2w volumes. The parameter set which yielded the lowest least-squares GRAPPA fit error to the calibration data was used as this has in our experience shown to correlate extremely well with the least amount of motion. The scalar error measure based on the residual error $(\mathbf{y} - \hat{\mathbf{y}})^2$ was defined as:

$$\varepsilon = \max(\mathbf{r}) < \mathbf{r} > ; \quad \begin{cases} r_{\text{slice}} = (\mathbf{y} - \hat{\mathbf{y}})^2 \\ \mathbf{r} = [r_{\text{slice}1}, \dots, r_{\text{slice}N}] \end{cases} \quad [1]$$

Phase correction (2), complex sum-of-squares reconstruction, and complex averaging was employed to improve the noise characteristics compared to conventional magnitude averaging. Upon completion, images were automatically sent back directly to both the image database and PACS. Prior to averaging the DWI data, retrospective 3D rigid-body realignment was performed on the magnitude data. Firstly, the T_2w and the DWI's were realigned separately (3). Secondly, a mutual information based 3D registration between the mean magnitude T_2w data and the mean magnitude DWI data (4) was conducted. Because, of the smaller head size and low SNR in the DWIs (Fig. 2a), it was necessary to use an 'importance weighting' of the data (we used one of the T_2w image volumes) for successful realignment of the DWI data. Third, the realignment parameters found were used to resample the real and imaginary parts of the data to retain the complex noise characteristics. All image reconstruction was performed using compiled threaded Matlab code on the vendor's multiprocessor reconstruction hardware.

The above 3D realignment procedure relies on that no motion occurs *within* a volume. While slice-to-volume image registration has been proposed (5), it is of little use for DWI where head motion tends to create massive artifacts over the entire slice (cf. Fig 2b). The main reason of doing DTI on patient A, was to try a new volume rejection criterion based on the residual error of the diffusion tensor summed over all voxels in the volume. Each DWI volume was assigned a value, ε , similar to Eq. 1, with the difference that $r_{\text{slice},i}$ is replaced with r_{voxel} and that \mathbf{r} contains all voxels in the DWI volume.

Results: In Fig. 1a, one slice of each of the leading five T_2w -w scans from Pat. A is shown. Inter-shot ghosting hampers the estimation of both ghost and GRAPPA parameters from the data. Applying these parameters on a motion free T_2w interleave later in the scan produces severe artifacts (Fig. 1b). However, with the aid of Eqn. 1, GRAPPA weights derived from the least motion hampered T_2w volume are used to produce artifact free data upon unfolding each shot in the data set (Fig. 1c). Figure 2 shows two realigned diffusion weighted volumes (no averaging) where patient is remaining still (a), and moves (b). Figures 3 and 4 show the isotropically DWI's with and without complex averaging, realignment and with 'good' and 'bad' GRAPPA weights. Note that FOV in Fig. 3 was much larger than here displayed.

Discussion & Conclusion: We have demonstrated on two unsedated children that high-quality diffusion imaging of the brain with high effective resolution is possible without using GA. With a new detection method (Eqn. 1) used to find both optimal GRAPPA weight sets and inferior DWI volumes, combined with a complete 3D rigid body realignment, phase correction and complex averaging as an integrated part of our reconstruction, highly diagnostic DWI data can now routinely be read on PACS within 10 minutes after the scan. With more processors, this time can be reduced further.

Acknowledgements: This work was supported in part by the NIH (2R01EB002711, 1R21EB006860, 1R01EB008706, and P41RR09784), Swedish Research Council (K2007-53P-20322-01-4), the Lucas foundation. Special thanks go to the MR technologists at the Lucille Packard Children's Hospital. A. White, S. Lim, M. Beers, A. Barikdar, Y. Chang and L. Ellison

References:

[1] Skare S et al. Magn Reson Med 2007;57(5):881-890. [2] Pipe J.G. et al. Magn Reson Med 2002;47(1):42-52. [3] Friston K. et al. Human Brain Mapping 1995;3:165-189. [4] Studholme C. et al.; 1998. SPIE. p 132. [5] Fei B. et al. Medical Imaging, IEEE Transactions on 2003;22(4):515-525

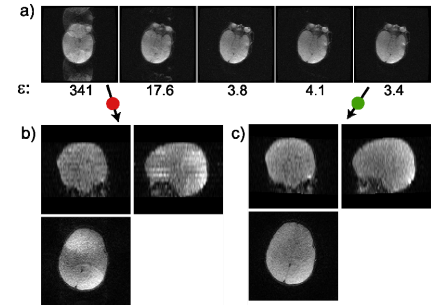


Figure 1 a) Based on ε , GRAPPA calibration on motion corrupted T_2w data can be avoided. b) Bad GRAPPA weights derived from motion corrupted volume cause artifacts, while motion free calibration data does not, c).

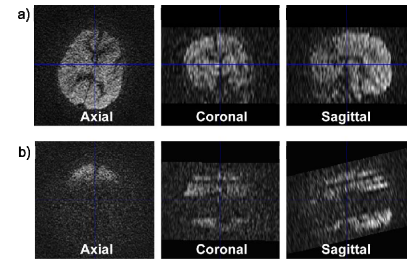


Figure 2 GRAPPA R=3 DWI (one direction, no averaging) on patient A post image realignment. a) DWI volume with no intra-volume motion. b) DWI volume with intra-volume motion, leading to erroneous 3D image realignment

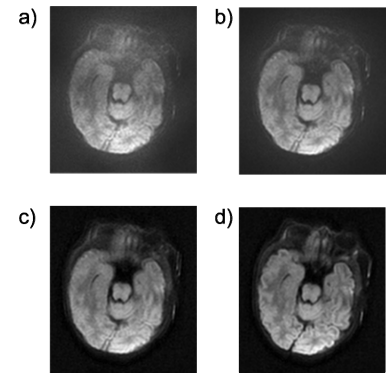


Figure 3 Isotropic DWI of Patient A. a) using GRAPPA weights from 1st T_2w volume and magnitude averaging. b) "optimal" GRAPPA weights, magnitude averaging. c) as b), but complex averaging. d) as c), after 3D realignment and bad volume rejection (displayed FOV cropped down to ~13 cm)

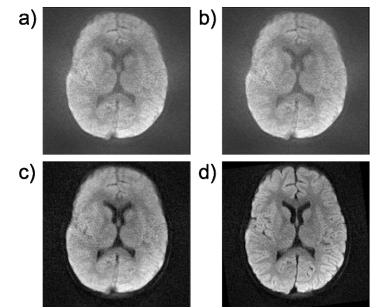


Figure 4 Isotropic DWI of Patient B. Same panel setup as in Fig. 3. Unlike Pat. A, this patient did not move right at the start of the scan, why the image quality in a) and b) are similar. The motion corrected and complex averaged data is given in d)